Spatio-temporal Reconstruction of dPET Data Using Complex Wavelet Regularisation*

Andrew McLennan and Michael Brady

Department of Engineering Science, University of Oxford, UK
andrew.mclennan@new.ox.ac.uk, jmb@robots.ox.ac.uk

Abstract. Traditionally, dynamic PET studies reconstruct temporally contiguous PET images using algorithms which ignore the inherent consistency between frames. We present a method which imposes a regularisation constraint based on wavelet denoising. This is achieved efficiently using the Dual Tree – Complex Wavelet Transform (DT-CWT) of Kingsbury, which has many important advantages over the traditional discrete wavelet transform: shift invariance, implicit measure of local phase, and directional selectivity. In this paper, we apply the decomposition to the full spatio-temporal volume and use it for the reconstruction of dynamic (spatio-temporal) PET data.

Instead of using traditional wavelet thresholding schemes we introduce a locally defined and empirically-determined Cross Scale regularisation technique. We show that wavelet based regularisation has the potential to produce superior reconstructions and examine the effect various levels of boundary enhancement have on the overall images.

We demonstrate that wavelet-based spatio-temporally regularised reconstructions have superior performance over conventional Gaussian smoothing in simulated and clinical experiments. We find that our method outperforms conventional methods in terms of signal-to-noise ratio (SNR) and Mean Square Error (MSE), and removes the need to post-smooth the reconstruction.

1 Introduction

Positron Emission Tomography (PET) is a functional medical imaging modality which is able to record accurate pharmacokinetic information. When a radiotracer such as ^{18}F-FDG is administered to the patient, the reconstruction of the detected projection data enables the visualisation of a tracer distribution in-vivo. Dynamic PET typically involves detecting and independently reconstructing a contiguous sequence of scans ("frames"), which can range in duration from a few seconds to many minutes. The choice of the specific frame duration is usually difficult to justify, with short frames having higher temporal resolution and long frames having higher spatial resolution. The majority of clinical PET scans

* We are thankful to Anthonin Reilhac for the use of PET-SORTEO; Siemens Molecular Imaging for providing clinical data; and the Department for Business Enterprise and Regulatory Reform for their financial assistance.

G.-Z. Yang et al. (Eds.): MICCAI 2009, Part II, LNCS 5762, pp. 398–405, 2009.

which have been performed to date are static in nature. However, in this work we show the potential improvements in image quality that are possible when the goal of dynamic imaging is explicitly incorporated into the reconstruction.

The main motivating factor of Dynamic PET over simple Static images is that abnormal physiology provides clinicians far more information than abnormal anatomy alone. This is particularly true for cancer radiotherapy treatment plans, where there is growing evidence that PET is able to visualise a patient's responsiveness to treatment before anatomical changes are apparent. Detecting early responses to treatment enables clinicians to modify treatment plans as required, reducing the patient's discomfort and improving their survival chance.

True signal recovery from noisy estimates is a classical signal analysis problem. Many attempts have been made to reduce the noise inherent in dynamic PET using various regularisation techniques. One idea is to apply Gaussian temporal filtering to smooth the Time Activity Curve (TAC) estimates. Another is the method of Nichols et al, which estimate TACs using B-Spline temporal basis functions [1]. Reader et al. proposed using a specific compartmental model [2]. Kamasak et al. [3] extended the idea of Carson and Lange [4] of directly estimating kinetic parameters from the projection data, but require that that compartmental model is known a priori. Various data-driven reconstruction methods have also been previously explored in the literature, such as PCA [5] and the KL transform [6].

Wavelet denoising has also been a popular topic in PET recently, with there being many attempts to remove noise from both the projection data as well as the reconstructed images. Shidhara et al. provides a good summary of a number of these methods with emphasis on how their application affects pharmacokinetic parameter estimates [7]. Lee et al. [8] utilises Robust Wavelet Shrinkage, Bhatia et al. [9] remodelled the FBP algorithm in the wavelet domain and Verhaeghe et al. recently proposed a reconstruction algorithm using E-Spline wavelet-like temporal basis functions [10].

The method we present explicitly incorporates a modified spatio-temporal wavelet regularisation procedure directly into the reconstruction algorithm. The method decomposes the spatio-temporal activity estimate into the complex wavelet domain and empirically regularises the reconstruction. The Dual Tree – Complex Wavelet Transform (DT-CWT) [11] is used due to its many superior properties. We show that our method results in improved dynamic PET reconstructions when tested on simulated data and leads to less noisy and visually improved images for clinical colorectal data.

2 Method

2.1 Image Reconstruction

The forward projection model of dynamic PET for a matrix of F temporal I-dimensional detected projection data vectors $\mathbf{Y} \sim \text{Poisson}\left\{\hat{\mathbf{Y}}\right\}$ can be written as:

$$\hat{\mathbf{Y}} = \mathbf{PX} + \mathbf{R} + \mathbf{S} \tag{1}$$

where $\mathbf{X}$ is the $J \times F$ spatio-temporal image activity matrix used to represent the dynamic radioactivity distributions; $\mathbf{P}$ is the forward projection matrix representing the probability that an emission from the j^{th} spatial basis function is detected by the i^{th} Line of Response (LOR); and $\mathbf{R}$ and $\mathbf{S}$ are the Randoms and Scatter contribution vectors to the expected data.

Substituting Equation (1) into the Log-Likelihood function of a Poisson process, differentiating and then rearranging gives the conventional ML-EM algorithm [12] for reconstructing the spatio-temporal tracer distribution $\mathbf{X}$:

$$\mathbf{X}^{k+1}(t) = \frac{\mathbf{X}^k(t)}{\mathbf{P}^T\mathbf{1}}\mathbf{P}^T\frac{\mathbf{Y}(t)}{\mathbf{P}\mathbf{X}^k(t) + \mathbf{R}(t) + \mathbf{S}(t)}, \tag{2}$$

where the product and division of vectors are understood to be carried out element-wise (as in [2]), $\mathbf{1}$ represents a vector of $1's$, and each temporal frame $t = 1, \cdots, F$ is reconstructed independently.

We modify the above algorithm to include spatio-temporal regularity between neighbouring voxels and temporal frames with the aim of preserving boundaries. After a single independent update of each of the F images using Equation (2), the reconstruction volume is decomposed, denoised and then recomposed using the multi-resolution complex wavelet transform. The overall regularised algorithm therefore becomes:

$$\mathbf{X}^{k+1}(t) = \frac{\tilde{\mathbf{X}}^k(t)}{\mathbf{P}^T\mathbf{1}}\mathbf{P}^T\frac{\mathbf{Y}(t)}{\mathbf{P}\tilde{\mathbf{X}}^k(t) + \mathbf{R}(t) + \mathbf{S}(t)} \tag{3}$$

$$\tilde{\mathbf{X}}^{k+1}(t) = \mathbf{W}\left(\mu\left(\mathbf{W}^{-1}\left(\mathbf{X}^{k+1}\right)\right)\right) \tag{4}$$

where $\mathbf{X}^k$ is the current reconstruction estimate for all time frames obtained from Equation (3), $\mathbf{W}$ and $\mathbf{W}^{-1}$ are the DT-CWT forward and inverse multi-resolution complex wavelet transforms, and μ is the denoising operator.

2.2 DT-CWT Cross Scale Regularisation

Gaussian Smoothing (GS) can be thought of as low-pass filtering in the frequency domain. Any high-frequency structures are assumed to be noise and smoothed regardless of their relative magnitudes. Wavelets on the other hand decompose signals into multi-resolution representations, based on scaled and translated "mother" wavelet functions. Compactly supported wavelets with large coefficients indicate jumps in signal value, whilst small absolute valued coefficients indicate mostly noise. This encodes important information at every resolution level in the coefficients on that level which have the largest absolute values. Keeping only these coefficients will result in less noisy reconstructions while ensuring edges remain sharp.

The Dual Tree – Complex Wavelet Transform (DT-CWT) of Kingsbury, which is documented in [11], is an efficient implementation of the complex-valued wavelet transform which has many advantageous properties over the traditional

Dyadic Discrete Wavelet Transform (DWT). For our work it can be considered a "black-box" which decomposes spatio-temporal volumes into multi-resolution complex coefficients. For a 1D signal, the complex valued wavelet coefficients are calculated by applying two separate standard DWT decompositions to the signal (with separate bio-orthogonal filters), with one tree containing the real coefficients and the other tree containing the imaginary coefficients.

The DT-CWT decomposition is shift invariant, directionally selective with strong orientation at multiple angles, has a measure of local phase[1] and is minimally redundant.[2] In this paper we use the advantageous properties of the DT-CWT and introduce a novel spatio-temporally varying denoising method aimed at being not only level dependent, but also adaptive to both varying signal and noise levels. We choose to use 3 decomposition levels and *near-symmetric* filters.

Conventional wavelet denoising methods usually consist of thresholding or shrinking wavelet coefficients with the aim of removing noise regardless of the signal's frequency content. The choice of particular threshold method and threshold value is in practice still an active area of research, and strongly influences the resulting images. Cross scale regularisation notes that edge information propagates across multiple frequencies, enabling an empirical level-dependent denoising scheme based on the boundary information from coarser levels.

Let F_w^l denote the multi-resolution complex wavelet decomposition for level l and directional sub-band w. Then, for each directional sub-band independently, and working from the second coarsest level to the finest, we pointwise multiply $\left|F_w^l\right|$ by the locally normalised coefficients of the next coursest level (performing interpolation where necessary):

$$M_l^{\text{new}} = \left|F_w^l\right| \cdot \frac{\left|F_w^{l+1}\right|}{(1-\alpha)\max\left\{\left|\left\{F_w^{l+1} \in N^3\right\}\right|\right\}}, \tag{5}$$

where N^3 is proportional to an eighth of the size of the current decomposition level and α is the boundary enhancement term used to amplify dominant coefficients. The use of an enhancement factor is somewhat ad hoc but its aim (and advantage) is to encourage sharper edges between regional boundaries[3]. Finally, we use the phase of the original complex wavelet coefficients to convert the new wavelet magnitudes back into the complex domain.

The denoising scheme proposed here is an extension to the conventional cross-scale method. It is able to account for the spatially varying noise levels found in PET reconstruction by working with local maximums, enabling boundaries for regions of any activity to be sharpened.

[1] It is well known that phase carries significant visual information and therefore should not be corrupted during the denoising process.

[2] TI-DWT of Coifman and Donoho is also shift-invariant but at the cost of being maximally redundant.

[3] We note that choosing α to be too large may result in imaging artefacts being produced due to the possible over amplification and dampening of voxel values either side of a boundary and hence we encourage erring on the side of caution when choosing the value.

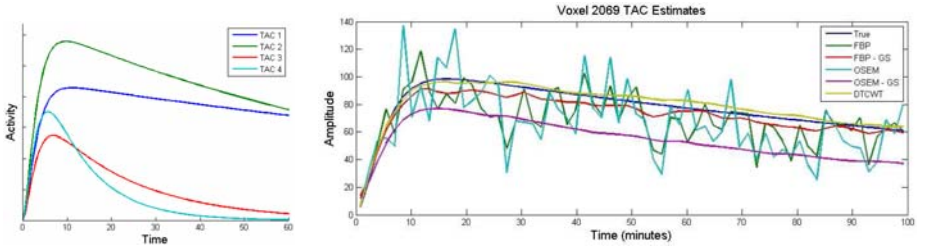

(a) Biologically plausible TACs (b) Example TACs estimates for the various reconstruction algorithms.

Fig. 1. Simulation TACs and reconstruction TAC estimates

3 Results and Discussion

The proposed DT-CWT denoising algorithm was assessed using both highly realistic 3D+t PET-SORTEO simulation data and clinical colorectal data. We compared our method to conventional FBP and OSEM, and a method which uses Gaussian Smoothing (GS) as opposed to Wavelet denoising. Many alternative reconstruction algorithms have previously been proposed but their clinical significance is less tried and tested. GS denotes the convolution of the current estimate with a spatio-temporal Gaussian kernel of size $\sigma = 1$.

3.1 PET-SORTEO Simulated 3D+t PET Data

The PET-SORTEO Monte Carlo-based simulator [13] is used to generate realistic dPET data based on the NCAT phantom. The biologically plausible TACs shown in Figure 1(a) taken from [2] were assigned to the four regions of the NCAT phantom shown in Figure 2. TAC 1 was assigned to the background, TAC 2 to the round anomalous region within the liver, TAC 3 to the liver and TAC4 to the round anomalous region in background.

Sixty four temporal frames each 93.75 seconds in duration were generated to produce sinograms of size $144 \times 288 \times 239$ covering the whole 1 hour 40 minute scan acquisition. A total of approximately 4.3 million events were recorded along the central slice through the phantom for which we show results. Randoms and Scatter events were not included in this simulation as, in the ideal case, they would be perfectly accounted for by the Randoms and Scatter matrices R and S respectively. Attenuation was also not simulated because it is assumed that this would be accounted for in practice using one of a variety of correction techniques. Images of size 64×64 were produced for reconstruction algorithms.

We compare the conventional reconstruction algorithms with our new method, after 10 iterations (8 subsets). Figure 1(b) shows (typical) example voxel TAC estimates for the different algorithms compared. We see that the un-regularised FBP and OSEM algorithms have greatly varying activity curves compared to

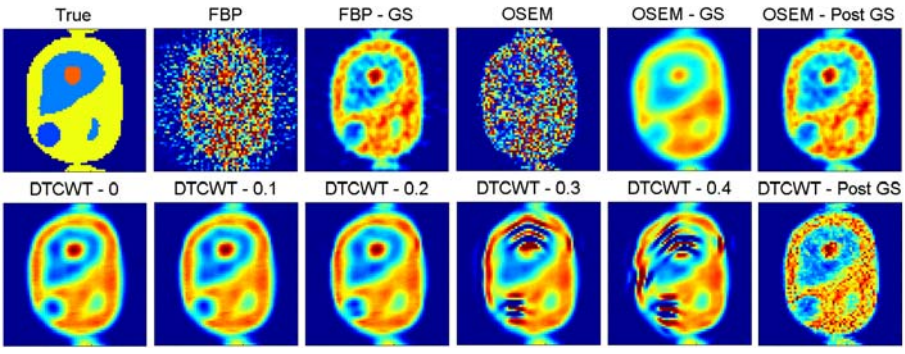

Fig. 2. Single central slice of frame 20 for different reconstructions. Top row: true image, FBP, FBP with post-Gaussian smoothing, OSEM, OSEM with inter-iteration GS and OSEM with post-GS. Bottom row: DT-CWT methods for enhancement levels 0, 0.1, 0.2, 0.3 and 0.4, and OSEM with post- DT-CWT denoising.

Table 1. Comparison of reconstruction algorithms: MSE and SNR

	MSE	ROI 1	ROI 2	ROI 3	ROI 4
FBP	66.35	3.511	4.767	-4.6114	-4.4709
FBP-GS	15.11	11.3985	11.5186	5.4651	**4.1076**
OSEM	52.67	2.3062	3.1173	-2.6621	-3.3012
OSEM-GS	13.79	11.5342	8.3733	4.0789	0.99131
OSEM- Post GS	12.48	11.6388	11.225	6.1949	**3.5224**
DT-CWT (0)	**10.02**	**11.6642**	**11.8975**	**6.2744**	2.9651
DT-CWT (0.1)	**10.04**	**11.6567**	**11.8726**	**6.3042**	3.0846
DT-CWT (0.2)	10.87	11.5011	11.7983	6.3400	2.7726
DT-CWT (0.3)	14.17	10.9838	9.0917	4.7827	1.3988
DT-CWT (0.4)	22.51	9.8971	4.3427	2.9892	0.54596
OSEM- Post DT-CWT	11.31	10.3631	9.6655	5.2576	2.8127

the regularise TACs. We note that the new method provides the best estimate out of all the algorithms, being not only lower in bias but temporally smoother.

Figure 2 shows the reconstructions of frame 20 for both conventional and our DT-CWT algorithms with five levels of enhancement. All of the regularised and smoothed images have reduced noise. Significant speckling remains for post reconstruction smoothing, however. The DT-CWT for small enhancement levels produces less noisy images with sharper edges between regions of interest. As expected, artefacts are introduced for large enhancement levels.

The quantitative accuracy of the reconstructions are compared by using the Mean Square Error (MSE) and Temporal Signal to Noise Ratio (TSNR) measures, taken from Verhaeghe et al [10]. Table 1 shows that the new method results in lower MSE than the conventional algorithms. Even though MSE is known not to be the best quantitative measure for medical imaging, it encourages further investigation. The average temporal SNR of each region shows that for the first

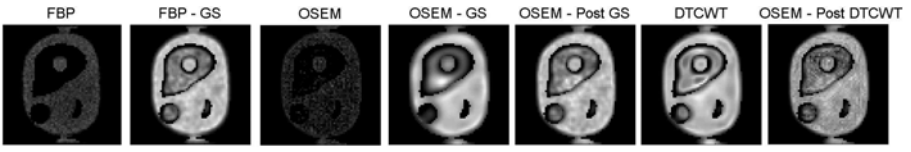

Fig. 3. Single central slice showing TSNR for the different reconstructions. Results shown for FBP (with and without post-GS), OSEM (with and without inter-iteration and post-GS), our DT-CWT method (with an enhancement level of 0.1) and OSEM with a single operation of post-reconstruction DT-CWT denoising.

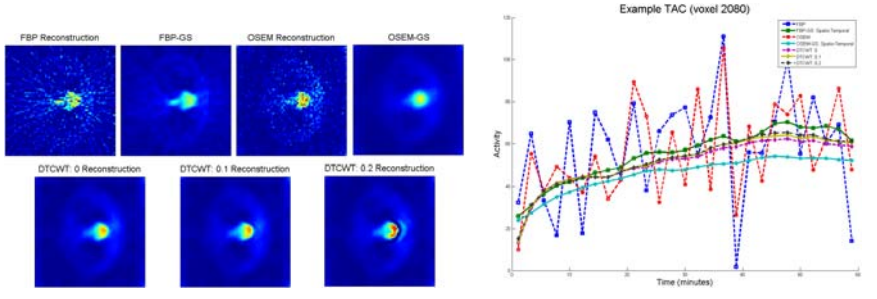

(a) Single central slice of frame 28 (b) Central voxel TACs

Fig. 4. FBP, FBP with post-GS, OSEM, OSEM with inter-iteration GS, and DT-CWT methods with enhancement levels 0, 0.1 and 0.2

three regions the new method out-performs the conventional methods. FBP with post-Gaussian smoothing results in larger TSNR for the last region, which we suspect is caused by slight biasing due to the region's proximity to the phantom's exterior. Figure 3 shows the TSNR values of each voxel in the 2D slice. We see that our DT-CWT with a boundary enhancement of 0.1 results in superior SNR around region edges than the OSEM-GS method and less speckling than post-Gaussian smoothing.

3.2 Clinical 3D+t Colorectal PET Data

To aid the validation process for the above new DT-CWT dynamic PET reconstruction technique we apply the algorithms to clinical colorectal data. A total of 321 million events where recorded for a 60 minute acquisition, acquired from Siemens Molecular Imaging. These events were then histogrammed into twenty eight equal duration contiguous sinograms of size $336 \times 336 \times 313$. Results are again shown for the 64×64 central slice reconstruction.

Figure 4(a) shows the reconstructions of the final frame (128 seconds of data) for the DT-CWT method with three levels of enhancement, FBP with and without post-Gaussian smoothing, and conventional OSEM with and without inter-iteration Gaussian smoothing. It appears that the DT-CWT method significantly reduces noise due to the spatio-temporal regularisation, but without overly blurring boundary edges seen in the OSEM-GS image. An enhancement

greater than zero again appears to lead to sharper images, but it needs to be small enough not to introduce artefacts. Figure 4(b) compares the TACs obtained by the various methods, demonstrating again that noise is reduced by the DT-CWT method.

4 Conclusion

A novel approach to dynamic PET iterative reconstruction is proposed which ensures consistency between neighbouring voxels and frames using DT-CWT. The method regularises the reconstruction process using spatio-temporal wavelet denoising. The Cross-Scale Regularisation method is examined and shown to lead to better results than Gaussian smoothing for our experiments. Results are shown for simulated and clinical dPET data and imply that wavelet regularisation enables superior quantitative reconstructions.

References

1. Nichols, T., Qi, J., Asma, E., Leahy, R.: Spatiotemporal Reconstruction of List Mode PET Data. Trans. Med. Imag. 23(4), 396–404 (2002)
2. Reader, A.J., Matthews, J.C., Sureau, F.C., Comtat, C., Trebossen, R., Buvat, I.: Iterative Kinetic Parameter Estimation within Fully 4D PET Image Reconstruction. IEEE Nuc. Sci. Symp. Conf. 3, 1752–1756 (2006)
3. Kamasak, M.E., Bouman, C.A., et al.: Direct Reconstruction of Kinetic Parameter Images from Dynamic PET Data. IEEE Tran. Med. Imag. 24(5), 636–650 (2005)
4. Carson, R., Lange, K.: The EM Parametric Image Reconstruction Algorithm. J. Am. Stat. Assoc. 80, 20–22 (1985)
5. Kao, C.M., Yap, J.T., Mukherjee, J., Wernick, M.N.: Image Reconstruction for Dynamic PET Based on Low-Order Approximation and Restoration of the Sinogram. IEEE Transactions on Medical Imaging 16(6), 738–749 (1997)
6. Wernick, M.N., Infusino, E.J., Milosevic, M.: Fast Spatio-Temporal Image Reconstruction for Dynamic PET. IEEE Trans. on Med. Imag. 18(3), 185–195 (1999)
7. Shidahara, M., Ikoma, Y., Kershaw, J., Kimura, Y., Naganawa, M., Watabe, H.: PET Kinetic Analysis: Wavelet Denoising of Dynamic PET Data with Application to Parametric Imaging. Ann. Nucl. Med. 21, 379–386 (2007)
8. Lee, N.Y., Choi, Y.: A Modified OSEM Algorithm for PET Reconstruction using Wavelet Processing. Comp. Meth. Prog. Biomed. 80(3), 236–245 (2005)
9. Bhatia, M., Karl, W.C., Willsky, A.S.: A Wavelet-based Method for Multiscale Tomographic Reconstruction. IEEE Trans. Med. Imag. 15(1), 92–101 (1996)
10. Verhaeghe, J., Ville, D.V., Khalidov, I., d'Asseler, Y., Lemahieu, I., Unser, M.: Dynamic PET Reconstruction Using Wavelet Regularization With Adapted Basis Functions. MedImg. 27(7), 943–959 (2008)
11. Selesnick, I.W., Baraniuk, R.G., Kingsbury, N.G.: The Dual-Tree Complex Wavelet Transform. IEEE Signal Processing Magazine 22(6), 123–151 (2005)
12. Shepp, L., et al.: Maximum Likelihood Reconstruction for Emission Tomography. Tran. Med. Imag. 1(2), 113–122 (1982)
13. Reilhac, A., Lartizien, C., et al.: PET-SORTEO: A Monte Carlo-based Simulator with High Count Rate Capabilities. IEEE Trans. Nuc. Sci. 51(1), 46–52 (2004)